RESEARCH ARTICLE

Facile assembly of an affordable miniature multicolor fluorescence microscope made of 3D-printed parts enables detection of single cells

Samuel B. Tristan-Landin☯, Alan M. Gonzalez-Suarez☯, Rocio J. Jimenez-Valdes, Jose L. Garcia-Cordero *

Unidad Monterrey, Centro de Investigación y de Estudios Avanzados del IPN, Parque PIIT, Apodaca, Nuevo León, Mexico

☯ These authors contributed equally to this work.
* jlgarciac@cinvestav.mx

🔓 OPEN ACCESS

Abstract

Fluorescence microscopy is one of the workhorses of biomedical research and laboratory diagnosis; however, their cost, size, maintenance, and fragility has prevented their adoption in developing countries or low-resource settings. Although significant advances have decreased their size, cost and accessibility, their designs and assembly remain rather complex. Here, inspired on the simple mechanism from a nut and a bolt, we report the construction of a portable fluorescence microscope that operates in bright-field mode and in three fluorescence channels: UV, green, and red. It is assembled in under 10 min from only six 3D printed parts, basic electronic components, a microcomputer (Raspberry Pi) and a camera, all of which can be readily purchased in most locations or online for US $122. The microcomputer was programmed in Python language to capture time-lapse images and videos. Resolution and illumination conditions of the microscope were characterized, and its performance was compared with a high-end fluorescence microscope in bright-field and fluorescence mode. We demonstrate that our miniature microscope can resolve and track single cells in both modes. The instructions on how to assemble the microscope are shown in a video, and the software to control it and the design files of the 3D-printed parts are freely available online. Our portable microscope is ideal in applications where space is at a premium, such as lab-on-a-chips or space missions, and can find applications in basic and clinical research, diagnostics, telemedicine and in educational settings.

Introduction

Fluorescence microscopy is an essential tool in biomedical research used to visualize, analyze and study molecules, cells and tissues. One of its main applications is to enable the quantification and localization of cellular components [1], which enables quantitative biology. Other important applications include its usage as a readout mechanism in biochemical assays such

immunoassays or quantitative polymerase chain reaction (qPCR). In the healthcare sector, fluorescence microscopy has been recommended by the World Health Organization for the diagnosis of tuberculosis [2]. However, because of its cost, training, maintenance and fragility, conventional fluorescence microscopes remain out of reach in developing countries, in rural areas and in remote settings [3–6]. Thus, access to affordable fluorescence microscopes (albeit at the cost of compromising certain functionalities and resolution) can facilitate its deployment in these settings and its usage in point-of-care diagnostics, telemedicine, and environmental monitoring, benefitting global healthcare. Furthermore, producing affordable and easy-to-assemble laboratory tools and instrumentation could facilitate research, produce quality results [7], improve laboratory productivity [8], and can potentially lead to new discoveries in biology, physiology, chemistry, and biomedicine [9,10].

Affordability and portability in fluorescence microscopy has been accomplished by retrofitting optical elements (objectives, filters, light emitting diodes, lasers, lenses, mirrors) and 3D-printed parts to smartphones cameras [3,5,11–13]. However, smartphones, although extremely powerful and unique, are difficult to reconfigure and take apart [14]; in addition, they evolve at a rapid pace, and constant software updates on their operating systems may disrupt their performance, making them obsolete [15]. Also, their size hampers further miniaturization and interferes in the integration with other add-ons or sensors, making them not ideal for long-term biological experimentation [16]. A different approach has been to use regular cameras (webcams or digital cameras) placed in a framework made of plastic parts, metallic hardware, and 3D-printed parts [5,6,16,17]; however, in some cases, the complexity of their designs encumbers downstream integration with other 3D printed parts. More importantly, the number of pieces needed to put it together may be overwhelming for a newcomer or for technologists trying to develop affordable instrumentation in low-resource settings. It also hampers its prompt adoption by scientists who are setting up a laboratory with limited resources and who need a multi-channel fluorescence microscope with basic functionalities and sufficient quality for most biological applications. Microscopes based on single-board computers and 3D printed parts have been reported, such as the OpenFlexure [18], but they lack the capability of fluorescence imaging.

To solve some of these issues, we introduce a portable, low-cost multicolor fluorescence microscope the size of a cube with a side length of 7 cm. Its operation and framework are inspired in the mechanism of a nut and a bolt. The microscope is assembled from only six 3D-printed parts, 4 power light-emitting diodes (LEDs), an eight-megapixel (MP) complementary metal–oxide–semiconductor (CMOS) camera, a metallic rod, and a Printed Circuit Board (PCB) with basic electronics. Aside from the Foldscope [19], which does not contain any camera sensor, our fluorescence microscope is assembled using the least amount of mechanical pieces (see **S2 Table** for a comparison with other different miniature microscopes). After pieces are 3D-printed and a PCB manufactured, the microscope can be assembled in 10 min (see **S1 Video**) with the capability to acquire images in bright-field and in three fluorescence channels. We present instructions for its assembly, characterization of its illumination homogeneity in each of the fluorescence channels, and demonstrate its operation in a cellular biological assay where it is possible to track single cells captured in microwells.

Materials and methods

3D-printed chassis

Microscope parts were designed in Inventor (ver 2017, Autodesk) and fabricated in a 3D printer (Makerbot Replicator 2); see **S1 Fig**. Dimensions of the microscope tube are shown in **S2 Fig**. The parts are made of black polylactic acid (PLA) and printed with the following

settings: speed in X and Y axis of 40 mm/s, temperature of 230˚C, layer thickness of 200 μm, and infill of 20%. Once fabricated, pieces were manually assembled; see **S1 Video** for a step-by-step assembly.

Electronics and optical components

The optical system relies on the Raspberry Pi Camera Module V2 that comes with an 8-Mega-Pixel CMOS image sensor camera and a plastic lens. This lens comes with the camera and no further specifications are provided on it; however, US Patent 7,564,635 B1 provides the description of a lens that has the same focal length (3.04 mm) that is provided in the specification of this camera module. High brightness LEDs (white, UV, green and blue) were used to illuminate the sample. Plastic color filters (Roscolux) or single-band pass optical filters (Zeiss) were used as emission filters and placed between the image sensor and the lens. A custom printed circuit board (PCB) containing the electronic components to control the LEDs were placed below the camera. The schematic and the list of components can be found in **S3 Fig** and **S1 Table**, respectively.

Graphical user interface (GUI)

A single-board microcomputer (Raspberry Pi 3 Model B) was used to program and control a graphical interface using Python 2.7 and OpenCV. The GUI allowed to acquire images and control the LEDs and different image parameters, such as the exposure time, brightness and contrast (**S4 Fig**).

Cell assays

To compare image quality acquired with our microscope and a conventional microscope, human monocytic (THP-1, kindly donated by Dr. Vianney Ortiz) cells were permeabilized with Tween-20 (P1379, Sigma Aldrich) 0.05% in Phosphate-Buffered Saline (PBS) 1X for 15 min, centrifuged at 1,200 rpm for 5 min, and washed with PBS 1X. Next, cells were incubated for 20 min either with 4′,6-diamidino-2-phenylindole (DAPI, 2.9 μM, 62247, Thermo Fisher Scientific) or Calcein-AM (20 μM, C1359, Sigma Aldrich), or for 10 min with Ethidium Homodimer (16 μM, EthD-1, E1903 Sigma Aldrich). The cells were washed again with PBS 1X and centrifuged at 1,200 rpm for 5 min. Then, 20 μL of the cellular suspensions were spread over three different clean coverslips and allowed to dry. Finally, 10 μL of glycerol were added and a second coverslip was placed on the top of the samples. For Calcein-AM staining, cells were not permeabilized, and PBS 1X was used instead of glycerol. Finally, coverslips were sealed with enamel.

Neutrophil assay

Purified neutrophils were donated by Dr. Alejandro Sánchez González (Blood donor informed consent and protocol was approved by the Research Ethics Committee of the Medicine Faculty and University Hospital of the Autonomous University of Nuevo León, Mexico, registered with the number MB19-00003). Briefly, human peripheral-blood neutrophils were purified from human blood by a non-continuous Percoll density gradient. After purification, neutrophils nuclei were stained with Hoechst 33342 (H3570, Thermo Fisher Scientific) at 16.2 μM for 5 min. Neutrophils were stimulated with either HBSS buffer 1X (control) or with *E. coli* lipopolysaccharide (LPS at 100 μg/mL, L2755, Sigma Aldrich). Both solutions contained Sytox Orange (S11368, Thermo Fisher Scientific) at 5 μM for nucleic acid staining. Devices made of polydimethylsiloxane (PDMS) were fabricated by soft-lithography and consisted of microwells

(20 μm diameter, 20 μm height). Cells were placed in three devices, one of them was placed on the stage of the miniature microscope with the stimulus solution and the other two on an inverted fluorescence microscope (Axio Observer, Zeiss). 20 μL of the cell suspension was added to the three devices. After 5 min, 20 μL of the stimulus were added to two devices, one in our microscope and the other in the Zeiss microscope. 20 μL of HBSS buffer was added to the other device sitting on the Zeiss microscope, which served as a negative control. Next, images in bright-field and red and blue fluorescence channels were acquired every 10 min in both microscopes. Images were analyzed using an image processing software (Fiji) where fluorescence intensity was measured over time for all individual microwells.

Cell tracking in a microfluidic device

A single-channel microfluidic device was designed in AutoCAD (Student version, Autodesk) and fabricated by soft-lithography [20]. The device consists of an inlet, an outlet, and a long serpentine channel with a height and width of 20 and 40 μm, respectively. The device was placed on the miniature microscope stage and a THP-1 cell suspension stained with Calcein-AM was flowed into the channel using a 1 mL syringe. The center of the device was focused, and a video was recorded in bright-field and in the green fluorescence channel while the cells were flowing through the serpentine channel.

THP-1 culture and time lapse microscopy

THP-1 cells (kindly donated by Dr. Vianney Ortiz), were incubated using supplemented RPMI-1640 medium (11875093, Thermo Fisher Scientific) inside a T25 flask before experimentation. A 1 mL chamber was fabricated using a PDMS slab, plasma bonded to a cover slide and exposed to ultraviolet (UV) light for 3 hours. 900 μL of fresh media was added to the chamber followed by 100 μL of THP-1 cell suspension at 100 x 10^5 cell/mL. Another block of PDMS was used to seal the chamber from the top. The cell chamber was placed on the miniature microscope stage and the whole microscope inside a cell culture incubator at 37°C with 5% CO_2. The bottom of the chamber was manually focused, and the miniature microscope was set in time-lapse mode on the GUI. Next, all cables were disconnected, except for the power cord. During the first ~24 hours, bright-field images were acquired every 15 min. For the last ~2 hours, images acquisition was set to every minute.

Results and discussion

Microscope design

Our goal was to engineer a miniature multicolor fluorescence microscope of simple design that could be quickly assembled with the least possible number of pieces (see S2 Table). It also had to offer sufficient accuracy to focus on microscopic objects while being mechanically stable and indifferent to vibrations; but also had to be assembled using 3D printed parts to make it affordable and deployable in low-resources settings. Importantly, our objective was not to develop a fluorescence microscope that offered the same illumination and image quality as commercial microscopes, but rather an easily assembled microscope and affordable for low-budget laboratories. It also had to offer good resolution and image quality for most biological applications, to enable quantitative biological measurements in bright-field and in fluorescence channels.

The microscope is inspired in the simple mechanism of a nut and bolt, Fig 1A. The bolt head serves as a base and as a casing to enclose the sensor camera, while the tip of the bolt holds the plastic lens, Fig 1B and 1C. The nut functions as a stage that fits on the threaded
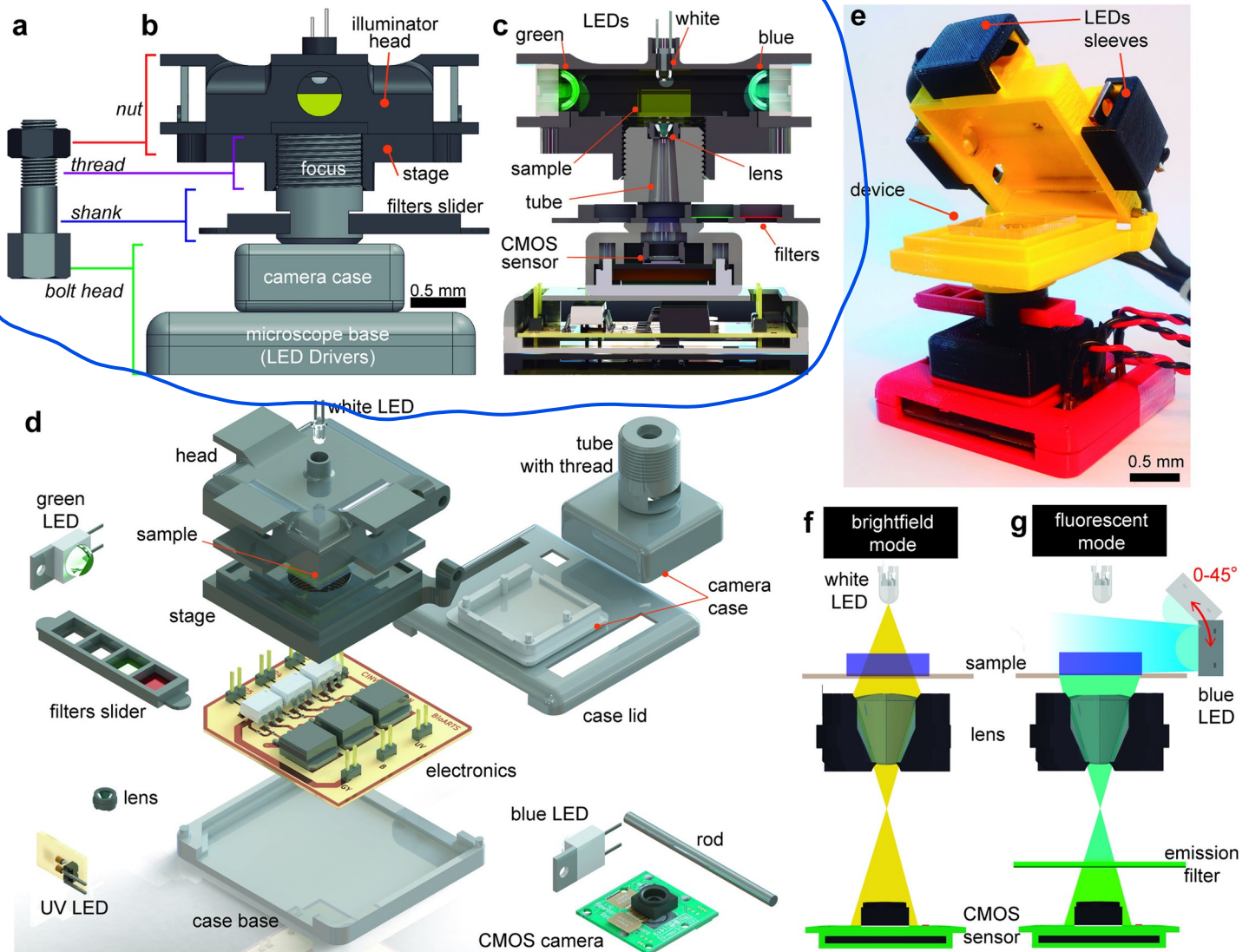
Fig 1. Anatomy of the miniature microscope. (**a**) The mechanism of the microscope is inspired by how a nut and bolt works. (**b**) Front view of the microscope. (**c**) Cutaway diagram of the microscope. (**d**) Exploded view of the different components comprising the microscope. (**e**) Photograph of the microscope with the lid open and a microfluidic device mounted on the stage. Schematic of the light path during operation of the microscope in (**f**) bright-field and (**g**) fluorescence mode. Color LEDs can be placed at different angles (0–45˚) to provide a homogeneous illumination.

https://doi.org/10.1371/journal.pone.0215114.g001

shank (1-mm threading; **S2 Fig**), but also supports the samples mounted on glass slides and serves as a lid for fluorescence observations (**Fig 1D**). The microscope base (bolt) is fixed while the stage rotates to bring the object into focus. It is important to realize that because the microscope is made of PLA, the threading on the nut and bolt can wear out over time (around 4 months) and thus decrease its ability to finely focus on microscopic objects. Nevertheless, the fabrication simplicity of these pieces, enables its easily replacement with new 3D printed parts for less than $1. One disadvantage of this arrangement is that the object under observation is rotated with the stage, yet once focused the object can be manually lifted from the stage and rotated to preserve the orientation.

Most fluorescence microscope configurations use fluorescence detection cubes (exciter, dichroic, and emitter) incorporated into a filter wheel. These detection cubes have excellent

optical qualities, but the cost for single-fluorescence channel filter cube can exceed a few hundred US dollars (see **S2 Table**), making them unsuitable for low-cost applications. Because LEDs have a very narrow band spectrum (20–40 nm), it is possible to omit the detection cube and just keep the emission filters. With these considerations, bright-field mode is enabled in our microscope using a white LED placed on the center top of the lid (**Fig 1E**), while fluorescence observations are achieved using 3 high-power color LEDs (UV: 385 nm, Blue: 475 nm, and Green:535 nm) that illuminate the sample from the sides (**Fig 1F**). Three plastic emission filters are placed on a hollowed-out tray that slides on the shank of the microscope, keeping one of the hollows empty for bright-field observations. However, it is possible to use regular microscope emission filters by modifying the dimensions of the tray and the shank. In summary, the simplicity of our configuration contrasts with other microscopes that require several 3D-printed parts [16,17,21].

Microscope parts

The microscope objective consists of a plastic lens detached from a commercial camera module and placed upside-down 25.4 mm above an 8 MP CMOS sensor (**Fig 1E**), in a similar configuration to what others have reported [16,22,23]. The sensor pixels contain three color pigment mosaic filters (Red, Green, Blue) that serve as extra emission filters by digitally extracting each channel from the raw image [16].

Our microscope is assembled from six 3D-printed pieces (a lid, a stage, a shank, front and back casing, and a tray), a metallic rod, 4 high-power LEDs, a CMOS camera, a lens, and an electronic control unit that powers the LEDs from a single 9V power supply, see **S1** and **S3 Figs**. The 3D printed pieces are fabricated in 2.5 hours while the microscope is assembled under 10 min. Instructions for the manual step-by-step assembly of the microscope are shown in **S1 Video**. Altogether, the size of the microscope is similar to a cube with a side length of ~7 cm and weighing only 58 g. The total cost of the opto-electro-mechanical system is $85 USD, see **S1 Table**. In comparison, a low-entry commercial microscope with a single fluorescence module can cost up to ~$1,900 and weight ~9.5 kg [4]. Because of its popularity and low-cost, we selected the microcomputer Raspberry Pi to control the microscope electronics and process the images. An added benefit of the Raspberry Pi platform is the plethora of plug-in sensors and accessories [14], together with the continuous software and hardware upgrades, that in the future could improve the capabilities of our microscope and aid in the automation of biological and biochemical assays. Adding the cost of the Raspberry Pi and the tablet, the total cost of our microscope increases to $202 USD.

Microscope operation

To operate the microscope, we created a graphical user interface (GUI) in Python 2.7 that allowed us to: (i) turn on and off the different color LEDs on demand, (ii) set the exposure time, (iii) capture still images, (iv) take videos or time-lapse images, and (v) save images in different formats, among other functions, **S4 Fig**.

Fig 2 shows the step-by-step operation of the microscope. It involves placing the sample on the stage by opening the lid. Next, the lid is closed to isolate the sample from external light sources. For bright-field observations, the white LED is turned on from the GUI and the tray is shifted to position the empty hole on the optical path. The stage is manually rotated clockwise or counterclockwise to focus the sample. For fluorescence observations, one of the color LEDs is turned on while the filter tray is manually slid to match the corresponding emission filter. **S2 Video** shows how easily the microscope is operated by a user.
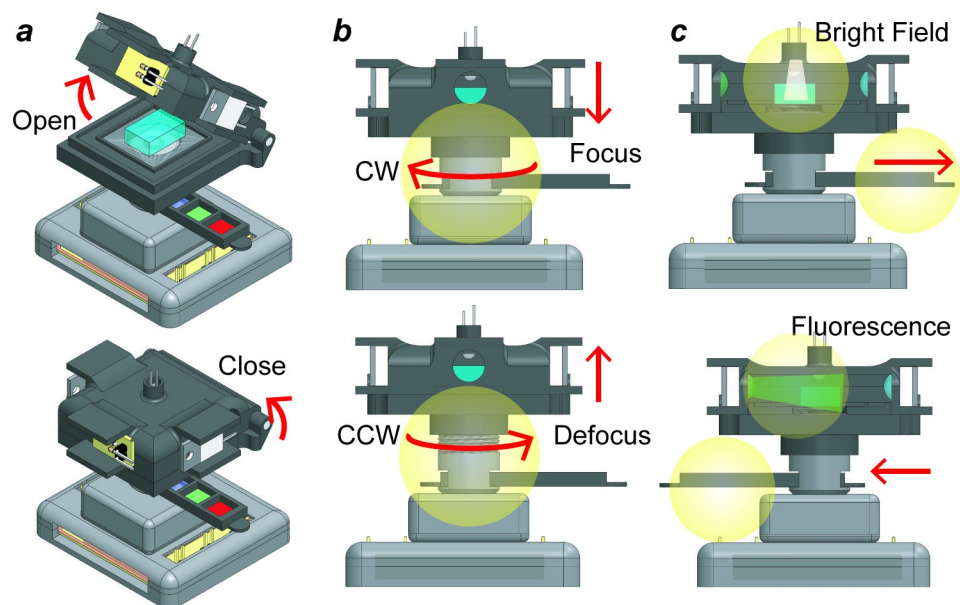
Fig 2. Step-by-step operation of the miniature microscope. (**a**) The lid is open to place a sample and then closed to prevent any external light sources to enter the stage and thus affect the image capture process. (**b**) Rotating the stage clockwise brings the sample closer to the lens, while rotating it counterclockwise moves the sample away from the lens. (**c**) To acquire bright-field or fluorescence images, the slider is moved manually either left or right to match the emission filter with the excitation LED. The leftmost hollow in the filter tray is kept empty for bright-field observation.
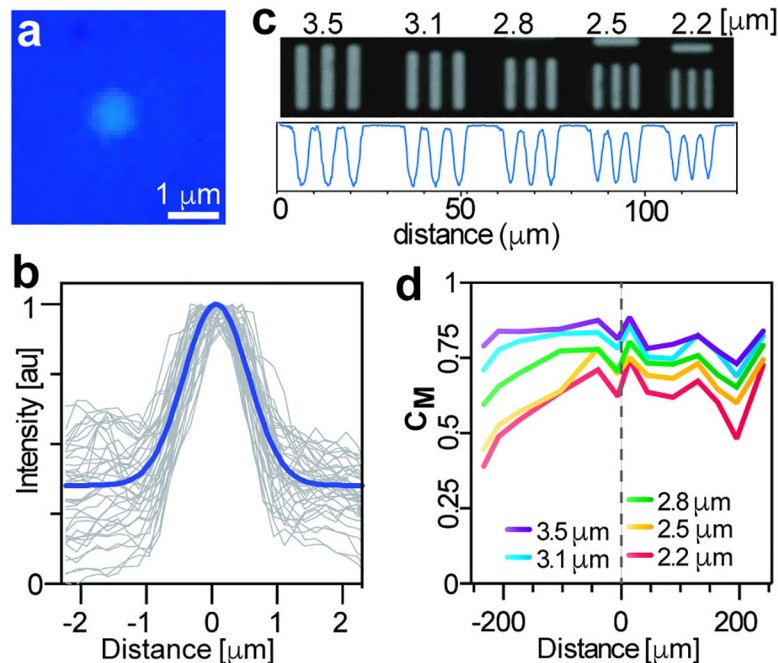
Fig 3. Tests to determine the resolution of the microscope. (**a**) Representative image of a 1 μm fluorescent bead. (**b**) Point spread functions of 40 1-μm beads with the blue line representing the average. (**c**) Bright-field images of the last 5 elements of group 7 on a 1951 USAF resolution target. Indicated on top is the thickness of each line. Below each image is the line profile as measured at halfway through all the lines. (**d**) Michelson contrast test using the same USAF target as measured across the width of the image. Gray dashed line represents the center of the image.

Microscope resolution

The theoretical magnification of our microscope is obtained using the magnification formula [24], considering that the object is located 3.5 mm away from the center of the lens and that the image is formed at a distance of 25.4 mm underneath the lens (where the CMOS sensor is located), resulting in 7x, almost identical to the value we obtained experimentally of 7.048x. It is important to highlight that adjusting the distance between the lens and the sensor leads to different magnifications. Because there are no eyepieces in our digital microscope and the image is displayed onto a monitor (510 x 384 pixels), the final total display magnification for digital microscopy is 257.3x, which is obtained by dividing the number of pixels for the monitor image width by the number of pixels for the sensor image width, and multiplying it by the pixel ratio [25].

The field of view is ~0.2 mm^2 (525 μm x 394 μm). According to the Rayleigh criteria, the theoretical optical resolution calculated at a wavelength of 550 nm is 0.448 μm. The focal length and working distance of the lens are ~3.05mm and ~0.1 mm, respectively. The lens has a numerical aperture of 0.45 and a depth of field of 1.46 μm. To determine the optical resolution of our system, we measured the full width at half maximum (FWHM) of the point spread function (PSF) for forty 1-μm fluorescent beads (Firefli Fluorescent Blue) spread over the whole field of view. The estimated FWHM of the 40 microbeads with our microscope is 1.187 μm, identical to the one obtained with a 20X objective using a Zeiss microscope, **Fig 3A and 3B**. We also imaged a 1951-USAF resolution target (R1DS1N, Thorlabs). As seen in **Fig 3C,** our microscope can clearly solve two lines separated by 2.2 μm. This is very similar to the calculated smallest resolvable line pair spacing of 2.05 μm, obtained by dividing the total display magnification (257.3x) by two times the monitor pixel size (0.264 mm) [25].

A common issue with custom-made microscopes is the radial loss of resolution farther from the center [22]. This is due to the alignment of the optical elements or the different pieces that comprise the microscope. Using the same USAF target, we measured the Michelson contrast (C_M, a measurement of contrast on gratings [26]), along the width of the field of view. An element is determined to be resolvable if $C_M \geq 0.1$ [22]. As shown in **Fig 3D**, the center of the image produces sharper contrasts for all the line sets, although there is a pronounced decreased of C_M values on the left side of the image, possibly due to the inclination of the sample stage of the microscope. Nevertheless, all the line sets of the USAF target produce a $C_M > 0.3$, even for patterns as small as 2.2 μm, a sufficient resolution for most cell-based measurements [6,13,16] and for the detection of some parasites [13].

Microscope illumination

To correct for uneven illumination intensity from light sources, fluorescence microscopes employ the Koehler illumination, a set of lenses positioned between the light source and the sample[27]. The simplest illumination correction systems to project LED light make use of collimator lenses [2], light-pipes, or elliptical mirrors [28] to generate a parallel beam, or in some cases a diffusor [17] or coupling prisms [2] to guide the beam, thus improving evenness of illumination but not fully correcting it [28]. Poor illumination translates into a poor contrast between the sample fluorescence and the background. However, adding these optical elements adds complexity, cost, and space to any microscopy system.

Thus, we wondered whether direct illumination, where the light source (without any optical elements) is placed near the sample, could give us a uniform illumination. This is a simpler and inefficient configuration as only a small percentage of the light produced by the LEDs reaches the sample [28], but because we used high-radiant power LEDs located very close to
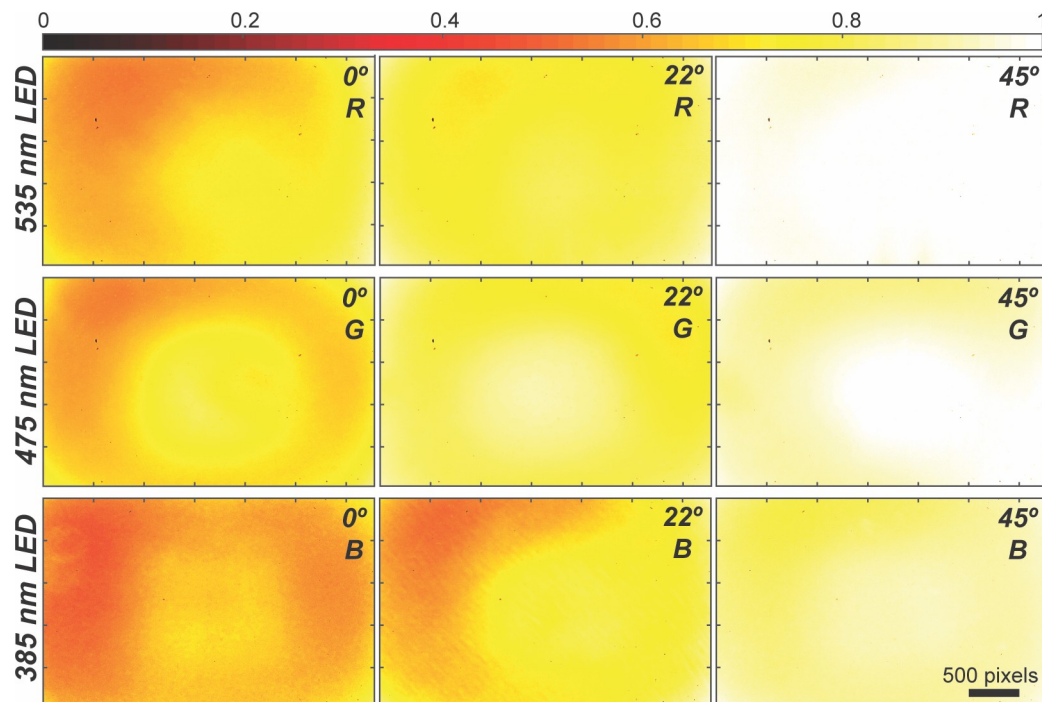
Fig 4. Effects of the angle position of the LEDs on the illumination uniformity using direct illumination. Each row corresponds to a different LED; the angle and the digital color channel analyzed are indicated on the top right corner. R: Red, G: Green, B: Blue. Fluorescence intensity has been normalized to a maximum value of 1.

https://doi.org/10.1371/journal.pone.0215114.g004

the sample, we hypothesized that this arrangement would still offer a workable illumination for most applications.

Because the color LEDs could not be placed on top of the sample, as it was already occupied by the white LED, the only positions left where the LEDs could be positioned were in the corners of the lid or at the cardinal points; we decided on the latter as it facilitated the mechanical design. We investigated how uniform was the illumination by illuminating fluorescent solutions (Hoechst, Fluorescein, and Rhodamine) at angles of 0°, 22° and 45° with a 1 s exposure times and employing the plastic filters (we fabricated three different lids to perform this experiment). **Fig 4** shows the heatmaps of the images captured by the CMOS color sensor at these different angles and considering only the digital channel closest to the emitted light. Data from the contribution of the rest of the RGB components can be found in **S5–S7 Figs**. As it can be observed, vignetting is appreciable in most cases, but it is more manifested at a 0° angle. However, as the angle increases to 22°, this vignetting is reduced, and almost eliminated for the red (R) channel and to a lesser extent on the green (G) channel, but is still significant for the blue (B) channel, noticing a reduced illumination on the left side of the heatmap, opposite to where the UV LED was placed. Increasing the angle to 45° reduces this vignetting for the B channel compared to the other angles; however, for the R channel the left side is less illuminated than the right side, while the G channel shows a higher radial darkening than at 22°. Emission detection on the other channels is highly attenuated but not completely blocked; this can be attributed to the poor optical quality of the plastic filters. Others [16] have reported that employing the color filter array (CFA) of the CMOS sensor is sufficient to block the excitation light; we did not found this possible, perhaps because of the quality of the CFA of our sensor. However, it is important to highlight that to improve image quality, color and dichroic glass filters can be fitted in our microscope. In general, the most suitable arrangement to get the

most even illumination in our microscope is for the UV LED to be located at an angle of 45°, and for both, the red and blue LEDs, placed at an angle of 22°. Note that this characterization would have to be performed if different LEDs are used, as they come with different lenses and sizes. In summary, a simple illumination configuration, in which the LEDs are placed in close proximity to the sample, can provide an illumination comparable to critical illumination [28].

Fluorescence images

To demonstrate the utility of our microscope to image single mammalian cells, we acquired bright-field and fluorescence images using plastic filters (<\$1) and optical glass filters (>\$100). **Fig 5A** shows micrographs of THP-1 cells stained with EthD-1 (ex/em 528/617 nm), Calcein-AM (ex/em 496/516 nm) and DAPI (ex/em 360/460 nm) using plastic filters. The intensity profile across the diameter of two cells for the three-fluorescence channels after subtracting background intensity is plotted in **Fig 5B**. As can be observed, plastic filters block fluorescence bleed-through from neighboring channels. Also, there is no significant difference with commercial glass filters, **S8 Fig**. This experiment demonstrated that our fluorescence microscope produces sufficient image quality to detect and analyze single cells.

Single-cell assay

To demonstrate the utility of our microscope in quantitative biological experiments, we performed a fluorescence time-lapse experiment to track the production of neutrophil extracellular traps (NETs) from single cells [29]. The nuclei of neutrophils isolated from peripheral blood were first stained with Hoechst, and then captured in a PDMS device containing an array of microwells (20 μm in diameter and depth). Next, cells were incubated with both LPS (to stimulate the production of NETs) and Sytox Orange (a DNA impermeant stain).
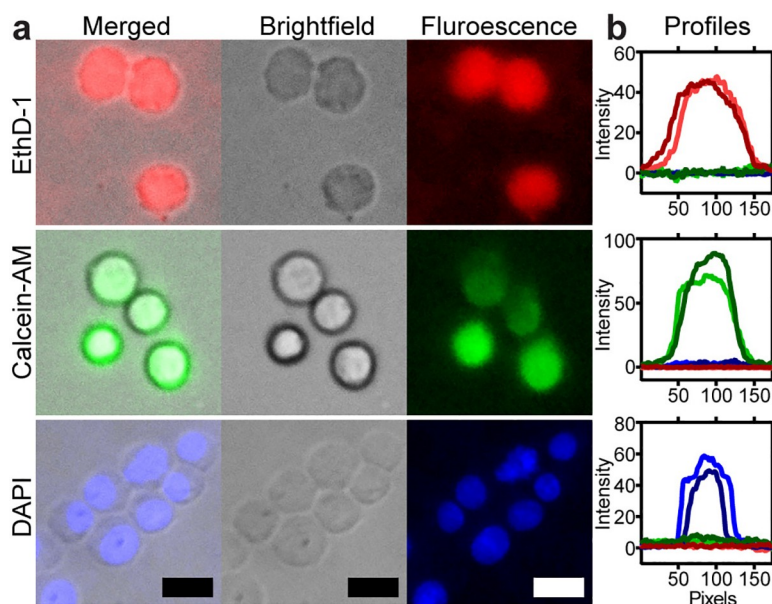

Fig 5. Fluorescence and bright-field micrographs of cells captured with our microscope. (**a**) Bright-field and fluorescence micrographs of THP-1 monocytes stained with three different fluorescent dyes. (**b**) Graphs show the fluorescence intensity profile across two cells in all channels; color represents the fluorescence contribution from each channel. From top to bottom, red, green, and blue fluorescence channel. Scale bar = 15 μm.
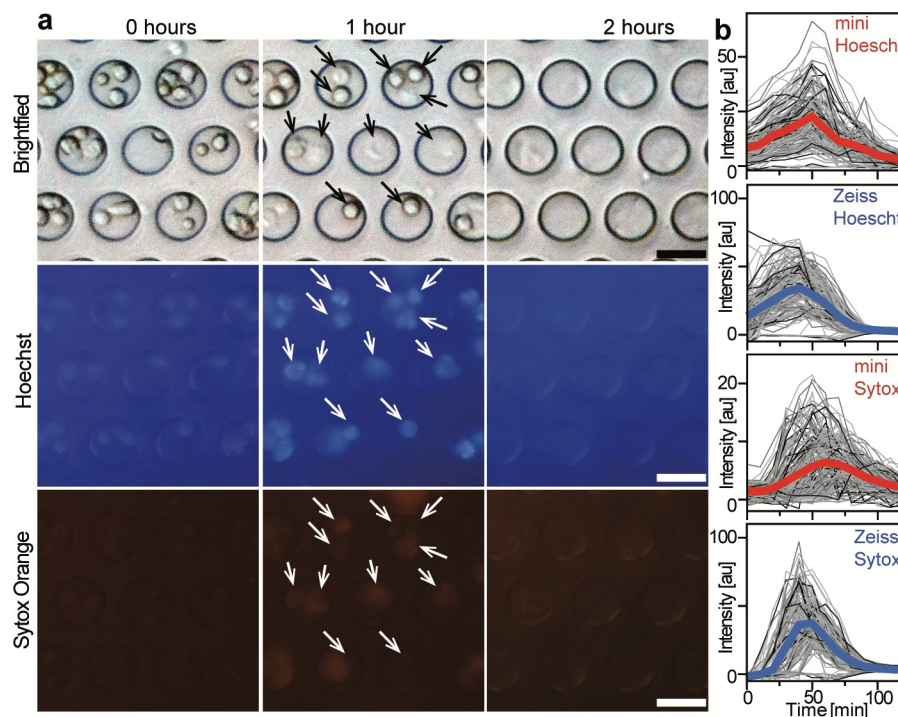
https://doi.org/10.1371/journal.pone.0215114.g005

Fig 6. Single cell assays in microwells. (**a**) Representative images of the neutrophil assay at different time points acquired with our microscope using plastic filters. Arrows point to single cells trapped in the microwells. Scale bar: 20 µm. (**b**) Traces of fluorescence intensities from single wells acquired with the miniature microscope (red) and a Zeiss microscope (blue). Thick lines represent the average of ~170 microwells.

https://doi.org/10.1371/journal.pone.0215114.g006

Bright-field and fluorescence images (UV and Red) were acquired every 10 min for 2 h with our microscope (shown in **Fig 6A**), and with a high-end inverted fluorescence microscope for comparison (not shown). As can be appreciated, it is possible to distinguish single cells trapped in each well. Analysis of individual wells captured with our microscope is shown in **Fig 6B**, where each gray trace corresponds to the fluorescence intensity of one individual well and the thick colored curves indicates the average of ~170 wells. The results for Sytox Orange with both microscopes have similar trends: in both cases, most of the wells showed a gradual increase in fluorescence intensity after ~15 min, reaching a peak at ~50 min (an indication of loss of plasma membrane integrity and thus yielding an indirect measurement of NETs formation), subsequently slowly decreasing as the DNA diffused out of the wells. In the case of Hoechst channel, the results of our microscope compare favorably to the Zeiss microscope, with both data showing a slight fluorescence intensity from the beginning of the assay—as all the cells nuclei were stained —increasing gradually to a maximum intensity at 50 min, to eventually decrease afterwards. A negative control experiment, where cells were incubated with Hank's solution, showed no change in fluorescence intensity over time, **S9 Fig**. The slight difference in the data obtained with the Zeiss microscope—higher peaks and smother curves—was expected given the high quality of its optical system, while ours had a higher background noise. Overall, it is possible to perform quantitative biological experiments in our microscope, enabling fluorescence time-lapse microscopy.

Cell tracking

Another feature of our miniature microscope is the capability to record video in bright-field and fluorescence mode. Using a single-channel microfluidic device with a width of 40 µm and

a height of 20 μm, we injected THP-1 cells stained with Calcein-AM at a speed of ~150 μm/s, and recorded a video while cells flowed through the channel (**Fig 7A and 7B**). **Fig 7C** shows a bright-field micrograph of a single cell flowing in the microfluidic channel, and **Fig 7D** shows fluorescence micrographs of two cells acquired with a 100 ms exposure time. **S3 Video** shows the facility to focus the optics onto the microfluidic channel and to start recording the cells flowing through the channel, demonstrating the capabilities of our fluorescence microscopy system to not only capture still images of objects sitting on a microscope slide.

Time-lapse microscopy in a cell culture chamber

Because of its size, one of the key features of our microscope is its portability, which enables to be used in different settings. To demonstrate this, we used the microscope inside a cell culture incubator set at 37˚C with 5% CO_2, and monitored the culture of THP-1 cells over 26 hours. **S10 Fig** shows a photograph of the miniature microscope placed inside the incubator and the PDMS chamber used for this experiment.

Fig 8A shows a series of bright-field micrographs captured every 15 min where cell migration and division can be appreciated. These images clearly show that cell proliferation can be observed without any disturbance inside the miniature microscope, proving its mechanical robustness. During the time lapse imaging, cells move around the field of view individually or even collectively, staying attached for a few hours after cell division. A sequence of micrographs captured every minute of cells undergoing cell division is shown in **Fig 8B** and **S4 Video**. It is evident that our microscope has enough resolution to observe: (i) the lamellipodia of cells extending and retracting, (ii) the migration of cells over time, and (iii) cells undergoing division.

Conclusions

Fluorescence microscopy is an important instrument in biomedical research. Here, we have demonstrated that using 3D printed parts and basic electronic components it is possible to build a miniature 3-channel fluorescence microscope for under $100. In our design, we
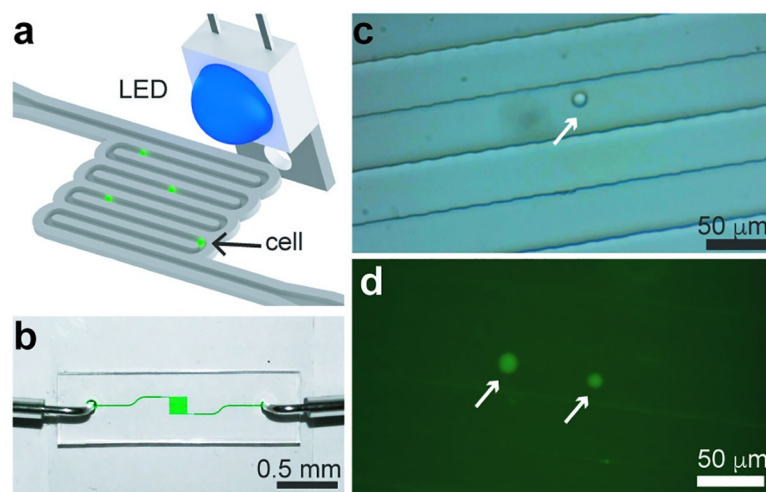

Fig 7. Tracking cells in a microfluidic channel. (**a**) Schematic of the microfluidic device in which cells stained with a fluorescent dye are flowed in a microfluidic device. (**b**) Photograph of the single-channel microfluidic device. (**c**) Bright-field image of a single THP-1 cell flowing at a speed of ~150 μm/s in a 40-μm wide channel. (**d**) Fluorescence micrographs of two cells flowing inside channel with a 100 ms exposure time. White arrows point to cells.
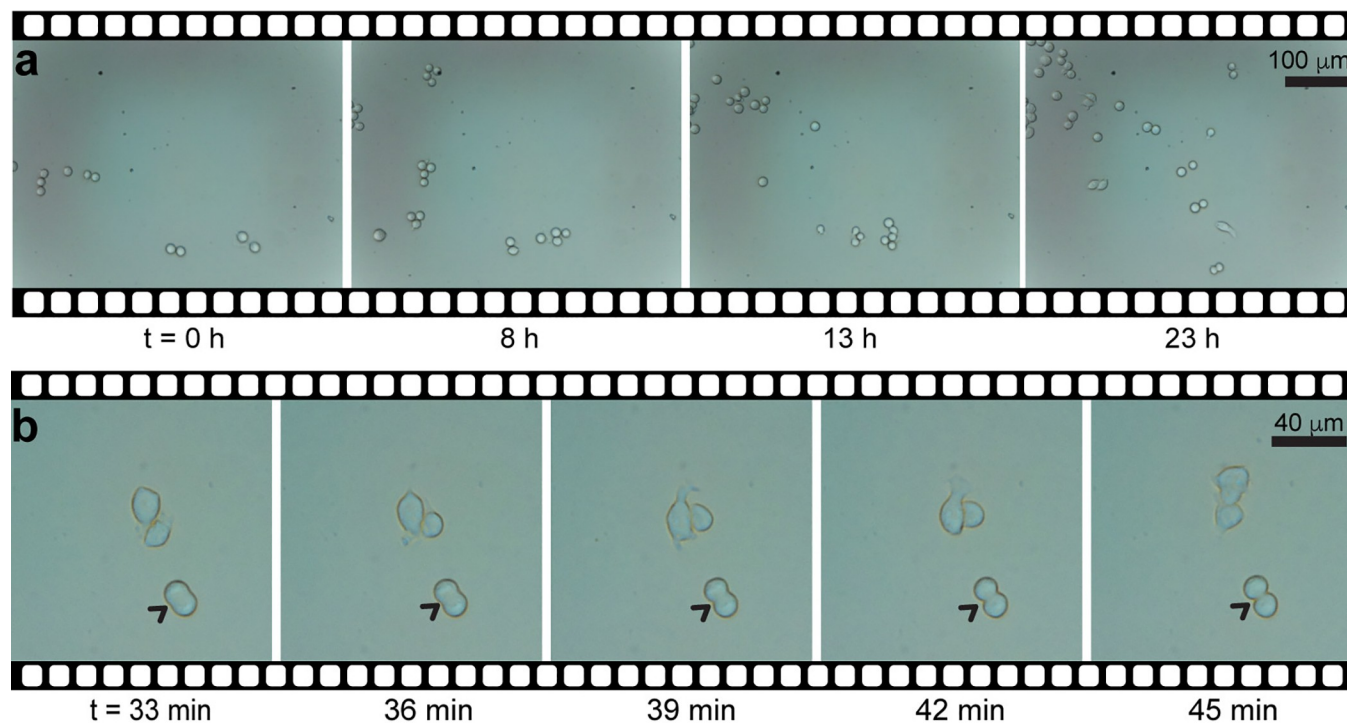
https://doi.org/10.1371/journal.pone.0215114.g007

Fig 8. Time-lapse imaging of THP-1 cells. (**a**) Sequence of bright-field micrographs of a cell culture assay that lasted 23 h; images were captured every 15 min. (**b**) Close-up to a sequence of images captured every minute showing the exact moment a cell is dividing (arrows).

https://doi.org/10.1371/journal.pone.0215114.g008

favored simplicity over other metrics so that it could be assembled rapidly (10 min), although still able to produce sufficient image quality to analyze single cells. We demonstrated that placing color LEDs at different angles from the sample produces a homogenous illumination. We also showed that plastic filters minimized fluorescence bleed-through to the same level of optical glass filters. To demonstrate its application in single cell assays, we monitored the production of NETs from single neutrophils, yielding similar data to a commercial microscope. Our microscope is ideal for downstream applications using microfluidic devices, as demonstrated here, or in situations where space is a premium (e.g. inside a CO_2 incubator), but we also foresee applications in diagnostics or telemedicine. Because of its low-cost and size, several microscopes could be assembled to monitor several assays at once.

Since LEDs have long-life spans (20,000–50,000 hours), our microscope is suitable for long-term experimentation which could enable acquisition of large amounts of data and translate into a better characterization of biological systems. One of the limitations of our microscope is its narrow field of view and its fixed magnification. Thus, an area of opportunity is to develop a motorized stage or use larger CMOS image sensors. Another limitation is the possible wear-out of 3D printed parts; however, all the microscope parts could be fabricated using sturdier materials, such as aluminum or other thermoplastics, using a variety of fabrication techniques. Albeit these limitations, our microscope performed a fluorescence time-lapse experiment of single cells yielding similar data to a conventional microscope.

Supporting information

S1 Table. Bill of materials used to build the microscope.
(PDF)

S2 Table. Comparison of the number of pieces required to assembly different DIY microscopes.
(PDF)

S1 Video. Web link to assembly of the microscope. https://github.com/BioARTS-Lab/
Miniature_Microscope/blob/master/Supporting%20Information/S1_Video.mpg.
(MPG)

S2 Video. Web link to operation of the microscope. https://github.com/BioARTS-Lab/
Miniature_Microscope/blob/master/Supporting%20Information/S2_Video.mpg.
(MPG)

S3 Video. Web link to tracking of cells flowing in a microfluidic channel. https://github.
com/BioARTS-Lab/Miniature_Microscope/blob/master/Supporting%20Information/S3_
Video.mpg.
(MPG)

S4 Video. Web link to time lapse of THP-1 cells growing on a flat surface. https://github.
com/BioARTS-Lab/Miniature_Microscope/blob/master/Supporting%20Information/S4_
Video.mpg.
(MPG)

S1 Fig. Photograph of the 3D-printed pieces used to assemble the miniature microscope.
(TIF)

S2 Fig. Design of the microscope tube. (Left) Front view of the mechanical tube of the microscope. Thread pitch is 1 mm. (Right) Cross-sectional view of the mechanical tube, showing the lens attached to the top of the tube. All dimensions are in mm.
(TIF)

S3 Fig. Schematic and PCB layout of the electronic control unit. (a) Circuit design. (b) Printed circuit board layout.
(TIF)

S4 Fig. Graphic User Interface (GUI) to control the microscope. The GUI was coded in Python by combining Tkinter, picamera and OpenCV libraries.
(TIF)

S5 Fig. Analysis of the illumination uniformity at an angle of 0˚ for all the channels. Each row corresponds to a different LED; the angle and the digital color channel analyzed are indicated on the top right corner. R: Red, G: Green, B: Blue. Fluorescence intensity has been normalized to a maximum value of 1.
(TIF)

S6 Fig. Analysis of the illumination uniformity at an angle of 22˚ for all the channels. Each row corresponds to a different LED; the angle and the digital color channel analyzed are indicated on the top right corner. R: Red, G: Green, B: Blue. Fluorescence intensity has been normalized to a maximum value of 1
(TIF)

S7 Fig. Analysis of the illumination uniformity at an angle of 45˚ for all the channels. Each row corresponds to a different LED; the angle and the digital color channel analyzed are indicated on the top right corner. R: Red, G: Green, B: Blue. Fluorescence intensity has been

normalized to a maximum value of 1
(TIF)

S8 Fig. Comparison of images captured with both microscopes. Bright-field and fluorescence micrographs captured with our microscope using plastic filters (left) or Zeiss filters (right). THP-1 cells stained with different fluorochromes: EthD-1 (red), Calcein-AM (green) and DAPI (blue). Images using all filters were acquired for each fluorochrome. Graphs show intensity profile of two cells across all channels, showing that there is no fluorescence bleed-through between channels.
(TIF)

S9 Fig. Negative control experiments. Traces of fluorescence intensities from single wells for the negative control experiment shown in Fig 6.
(TIF)

S10 Fig. Assay inside a cell culture incubator. (a) Photograph of the inside of a cell culture incubator showing the microscope and the microcomputer Raspberry. (b) Photograph of the cell culture chamber made of PDMS.
(TIF)

Acknowledgments

Author Contributions

Conceptualization: Samuel B. Tristan-Landin, Jose L. Garcia-Cordero.

Formal analysis: Samuel B. Tristan-Landin, Alan M. Gonzalez-Suarez, Rocio J. Jimenez-Valdes.

Funding acquisition: Jose L. Garcia-Cordero.

Investigation: Samuel B. Tristan-Landin, Alan M. Gonzalez-Suarez.

Methodology: Samuel B. Tristan-Landin, Alan M. Gonzalez-Suarez, Rocio J. Jimenez-Valdes, Jose L. Garcia-Cordero.

Project administration: Jose L. Garcia-Cordero.

Resources: Jose L. Garcia-Cordero.

Software: Samuel B. Tristan-Landin, Alan M. Gonzalez-Suarez.

Supervision: Alan M. Gonzalez-Suarez, Jose L. Garcia-Cordero.

Validation: Alan M. Gonzalez-Suarez.

Writing – original draft: Samuel B. Tristan-Landin, Alan M. Gonzalez-Suarez, Jose L. Garcia-Cordero.

Writing – review & editing: Samuel B. Tristan-Landin, Alan M. Gonzalez-Suarez, Rocio J. Jimenez-Valdes, Jose L. Garcia-Cordero.

References

1. Agard DA, Hiraoka Y, Shaw P, Sedat JW. Chapter 13 Fluorescence Microscopy in Three Dimensions. Methods in Cell Biology. 1989. pp. 353–377. https://doi.org/10.1016/s0091-679x(08)60986-3 PMID: 2494418

2. Wessels JT, Pliquett U, Wouters FS. Light-emitting diodes in modern microscopy-from David to Goliath? Cytom Part A. 2012; 81A: 188–197. https://doi.org/10.1002/cyto.a.22023 PMID: 22290727

3. Breslauer DN, Maamari RN, Switz NA, Lam WA, Fletcher DA. Mobile Phone Based Clinical Microscopy for Global Health Applications. Pai M, editor. PLoS One. 2009; 4: e6320. https://doi.org/10.1371/journal.pone.0006320 PMID: 19623251

4. Miller AR, Davis GL, Oden ZM, Razavi MR, Fateh A, Ghazanfari M, et al. Portable, Battery-Operated, Low-Cost, Bright Field and Fluorescence Microscope. Doherty TM, editor. PLoS One. 2010; 5: e11890. https://doi.org/10.1371/journal.pone.0011890 PMID: 20694194

5. Schaefer S, Boehm SA, Chau KJ. Automated, portable, low-cost bright-field and fluorescence microscope with autofocus and autoscanning capabilities. Appl Opt. 2012; 51: 2581. https://doi.org/10.1364/AO.51.002581 PMID: 22614477

6. Jin D, Wong D, Li J, Luo Z, Guo Y, Liu B, et al. Compact Wireless Microscope for In-Situ Time Course Study of Large Scale Cell Dynamics within an Incubator. Sci Rep. 2015; 5: 18483. https://doi.org/10.1038/srep18483 PMID: 26681552

7. Coloma J, Harris E. Innovative low cost technologies for biomedical research and diagnosis in developing countries. BMJ. 2004; 329: 1160–1162. https://doi.org/10.1136/bmj.329.7475.1160 PMID: 15539673

8. Sulkin MS, Widder E, Shao C, Holzem KM, Gloschat C, Gutbrod SR, et al. Three-dimensional printing physiology laboratory technology. Am J Physiol Circ Physiol. 2013; 305: H1569–H1573. https://doi.org/10.1152/ajpheart.00599.2013 PMID: 24043254

9. Bishop GW, Satterwhite-Warden JE, Kadimisetty K, Rusling JF. 3D-printed bioanalytical devices. Nanotechnology. 2016; 27: 284002. https://doi.org/10.1088/0957-4484/27/28/284002 PMID: 27250897

10. Symes MD, Kitson PJ, Yan J, Richmond CJ, Cooper GJT, Bowman RW, et al. Integrated 3D-printed reactionware for chemical synthesis and analysis. Nat Chem. 2012; 4: 349–354. https://doi.org/10.1038/nchem.1313 PMID: 22522253

11. Hernández Vera R, Schwan E, Fatsis-Kavalopoulos N, Kreuger J. A Modular and Affordable Time-Lapse Imaging and Incubation System Based on 3D-Printed Parts, a Smartphone, and Off-The-Shelf Electronics. Doh J, editor. PLoS One. 2016; 11: e0167583. https://doi.org/10.1371/journal.pone.0167583 PMID: 28002463

12. Wei Q, Qi H, Luo W, Tseng D, Ki SJ, Wan Z, et al. Fluorescent Imaging of Single Nanoparticles and Viruses on a Smart Phone. ACS Nano. 2013; 7: 9147–9155. https://doi.org/10.1021/nn4037706 PMID: 24016065

13. Zhu H, Yaglidere O, Su T-W, Tseng D, Ozcan A. Cost-effective and compact wide-field fluorescent imaging on a cell-phone. Lab Chip. 2011; 11: 315–322. https://doi.org/10.1039/c0lc00358a PMID: 21063582

14. Cressey D. The DIY electronics transforming research. Nature. 2017; 544: 125–126. https://doi.org/10.1038/544125a PMID: 28383014

15. Wang Z, Boddeda A, Parker B, Samanipour R, Ghosh S, Menard F, et al. A High-Resolution Minimicroscope System for Wireless Real-Time Monitoring. IEEE Trans Biomed Eng. 2018; 65: 1524–1531. https://doi.org/10.1109/TBME.2017.2749040 PMID: 28880156

16. Zhang YS, Ribas J, Nadhman A, Aleman J, Selimović Š, Lesher-Perez SC, et al. A cost-effective fluorescence mini-microscope for biomedical applications. Lab Chip. 2015; 15: 3661–3669. https://doi.org/10.1039/c5lc00666j PMID: 26282117

17. Maia Chagas A, Prieto-Godino LL, Arrenberg AB, Baden T. The €100 lab: A 3D-printable open-source platform for fluorescence microscopy, optogenetics, and accurate temperature control during behaviour of zebrafish, Drosophila, and Caenorhabditis elegans. PLOS Biol. 2017; 15: e2002702. https://doi.org/10.1371/journal.pbio.2002702 PMID: 28719603

18. Sharkey JP, Foo DCW, Kabla A, Baumberg JJ, Bowman RW. A one-piece 3D printed flexure translation stage for open-source microscopy. Rev Sci Instrum. 2016; 87: 025104. https://doi.org/10.1063/1.4941068 PMID: 26931888

19. Cybulski JS, Clements J, Prakash M. Foldscope: Origami-Based Paper Microscope. Martens L, editor. PLoS One. 2014; 9: e98781. https://doi.org/10.1371/journal.pone.0098781 PMID: 24940755

20. Gonzalez-Suarez AM, Peña-del Castillo JG, Hernández-Cruz A, Garcia-Cordero JL. Dynamic Generation of Concentration- and Temporal-Dependent Chemical Signals in an Integrated Microfluidic Device for Single-Cell Analysis. Anal Chem. 2018; 90: 8331–8336. https://doi.org/10.1021/acs.analchem.8b02442 PMID: 29916698

21. Nuñez I, Matute T, Herrera R, Keymer J, Marzullo T, Rudge T, et al. Low cost and open source multi-fluorescence imaging system for teaching and research in biology and bioengineering. Gilestro GF, editor. PLoS One. 2017; 12: e0187163. https://doi.org/10.1371/journal.pone.0187163 PMID: 29140977

22. Switz NA, D'Ambrosio M V., Fletcher DA. Low-Cost Mobile Phone Microscopy with a Reversed Mobile Phone Camera Lens. Pai M, editor. PLoS One. 2014; 9: e95330. https://doi.org/10.1371/journal.pone.0095330 PMID: 24854188

23. Kim SB, Koo K, Bae H, Dokmeci MR, Hamilton G a, Bahinski A, et al. A mini-microscope for in situ monitoring of cells. Lab Chip. 2012; 12: 3976–82. https://doi.org/10.1039/c2lc40345e PMID: 22911426

24. Jewett JW., Serway RA. Image Formation. Physics for Scientists and Engineers with Modern Physics. 7th ed. Cengage Learning EMEA; 2008. pp. 1008–1050.

25. DeRose JA, Doppler M. Guidelines for Understanding Magnification in the Modern Digital Microscope Era. Micros Today. 2018; 26: 20–33. https://doi.org/10.1017/S1551929518000688

26. Peli E. Contrast in complex images. J Opt Soc Am A. 1990; 7: 2032. https://doi.org/10.1364/JOSAA.7.002032 PMID: 2231113

27. Taylor DL. Chapter 13 Basic Fluorescence Microscopy. Methods in Cell Biology. 1988. pp. 207–237. https://doi.org/10.1016/S0091-679X(08)60196-X

28. Bosse JB, Tanneti NS, Hogue IB, Enquist LW. Open LED Illuminator: A Simple and Inexpensive LED Illuminator for Fast Multicolor Particle Tracking in Neurons. Anderson KI, editor. PLoS One. 2015; 10: e0143547. https://doi.org/10.1371/journal.pone.0143547 PMID: 26600461

29. Jimenez-Valdes RJ, Rodriguez-Moncayo R, Cedillo-Alcantar DF, Garcia-Cordero JL. Massive Parallel Analysis of Single Cells in an Integrated Microfluidic Platform. Anal Chem. 2017; 89: 5210–5220. https://doi.org/10.1021/acs.analchem.6b04485 PMID: 28406613